Published in final edited form as:
Neuron. 2012 September 6; 75(5): 810–823. doi:10.1016/j.neuron.2012.07.007.

Signal-mediated, AP-1/Clathrin-dependent Sorting of Transmembrane Receptors to the Somatodendritic Domain of Hippocampal Neurons

Ginny G. Farías, **Loreto Cuitino**, **Xiaoli Guo**, **Xuefeng Ren**, **Michal Jarnik**, **Rafael Mattera**, and **Juan S. Bonifacino***
Cell Biology and Metabolism Program, *Eunice Kennedy Shriver* National Institute of Child Health and Human Development National Institutes of Health, Bethesda, MD 20892, USA

SUMMARY

Plasma membranes of the somatodendritic and axonal domains of neurons are known to have different protein compositions, but the molecular mechanisms that determine this polarized protein distribution remain poorly understood. Herein we show that somatodendritic sorting of various transmembrane receptors in rat hippocampal neurons is mediated by recognition of signals within the cytosolic domains of the proteins by the μ1A subunit of the adaptor protein-1 (AP-1) complex. This complex, in conjunction with clathrin, functions in the neuronal soma to exclude somatodendritic proteins from axonal transport carriers. Perturbation of this process affects dendritic spine morphology and decreases the number of synapses. These findings highlight the primary recognition event that underlies somatodendritic sorting and contribute to the evolving view of AP-1 as a global regulator of cell polarity.

INTRODUCTION

Neurons are anatomically and functionally polarized cells that conduct nerve impulses in a vectorial fashion. Impulses are received by dendrites, propagated through the soma, and eventually transmitted by axons. To accomplish these specialized functions, the plasma membrane of each of these domains possesses a distinct set of transmembrane proteins, including receptors, channels, transporters and adhesion molecules (Horton and Ehlers, 2003; Lasiecka and Winckler, 2011). Although much has been learned about the signaling and cytoskeletal processes that contribute to the establishment of neuronal polarity (Arimura and Kaibuchi, 2005), the molecular mechanisms that underlie the biosynthetic sorting of transmembrane proteins to the different neuronal domains remain poorly understood (Horton and Ehlers, 2003; Lasiecka and Winckler, 2011).

Polarized sorting likely involves recognition of specific determinants within the transmembrane proteins by a molecular machinery that directs transport to different plasma membrane domains. Because sorting to the dendrites and soma often share a common mechanism, these compartments are jointly referred to as the “somatodendritic” domain (Horton and Ehlers, 2003; Lasiecka and Winckler, 2011). Dotti and Simons (1990) first demonstrated a correlation between sorting of transmembrane proteins to the

*Corresponding author, Tel: 301-496-6368, Fax: 301-402-0078, juan@helix.nih.gov.

somatodendritic and axonal domains of neurons and the basolateral and apical domains of polarized epithelial cells, respectively, suggesting that polarized sorting in these cell types has a similar underlying mechanism (Dotti and Simons, 1990). This correlation has held for many transmembrane proteins (Horton and Ehlers, 2003; Lasiecka and Winckler, 2011), although exceptions have also been reported (*e.g.*, Silverman et al., 2005; Jareb and Banker, 1998).

The determinants for biosynthetic sorting of transmembrane proteins to the apical/ axonal domains are diverse and not precisely defined. Much better understood are the determinants for sorting to the basolateral surface of epithelial cells. These determinants are generally present in the cytosolic domains of the proteins and in some cases consist of tyrosine-based, YXXØ-type, or dileucine-based, [DE]XXXL[LI]-type motifs similar to those that mediate rapid internalization from the cell surface and targeting to lysosomes (X represents any amino acid and Ø a bulky hydrophobic amino acid) (Bonifacino and Traub, 2003; Gonzalez and Rodriguez-Boulan, 2009). Other basolateral sorting determinants comprise amino acid residues that do not fit any known consensus motif, pointing to an additional role for non-canonical sequences in this process (Gonzalez and Rodriguez-Boulan, 2009). In general, YXXØ and [DE]XXXL[LI] signals are recognized by heterotetrameric adaptor protein (AP) complexes (*i.e.*, AP-1, AP-2 and AP-3) that are components of clathrin coats (Bonifacino and Traub, 2003; Robinson, 2004). In line with this notion, sorting of various transmembrane proteins to the basolateral surface of polarized epithelial cells has been shown to depend on AP-1 (Folsch et al., 1999; Gan et al., 2002; Gravotta et al., 2012; Carvajal-Gonzalez et al., 2012) and clathrin (Deborde et al., 2008). AP-1 localizes to the *trans*-Golgi network (TGN) and/ or recycling endosomes (RE) and is composed of four subunits (*i.e.*, "adaptins") named γ, β1, μ1 and σ1, some of which occur as two or three isoforms encoded by different genes (Boehm and Bonifacino, 2001; Mattera et al., 2011). An epithelial-specific isoform of μ1 termed μ1B (Ohno et al., 1999) is particularly important for the basolateral sorting of a variety of transmembrane proteins (Folsch et al., 1999; Gan et al., 2002) through recognition of both canonical and non-canonical signals (Gravotta et al., 2012; Carvajal-Gonzalez et al., 2012). Several studies have shown that somatodendritic sorting of transmembrane proteins in rat hippocampal neurons is also dependent on determinants present within the cytosolic domains of the proteins (Lasiecka and Winckler, 2011, and references therein). However, these determinants are less well defined than basolateral sorting signals (Lasiecka and Winckler, 2011). Moreover, neurons do not express μ1B but the ubiquitous μ1A isoform (Ohno et al., 1999). Studies in *C. elegans* have nonetheless shown that the ubiquitously-expressed μ1 ortholog UNC-101 is required for dendritic localization of several transmembrane proteins (Dwyer et al., 2001; Bae et al., 2006; Margeta et al., 2009).

In this study, we have examined the mechanisms of somatodendritic sorting in cultured rat hippocampal neurons with a focus on signal-adaptor interactions. We find that tyrosine-based sorting signals in the cytosolic domains of the transferrin receptor (TfR) and the Coxsackievirus and adenovirus receptor (CAR) mediate sorting to the somatodendritic domain. Both signals bind with distinct sequence requirements to the μ1A subunit of AP-1. Using dominant-negative overexpression and RNAi approaches, we show that signal recognition by μ1A, as well as the whole AP-1 complex and clathrin, are required for sorting of these transmembrane cargos to the somatodendritic domain. Microscopic imaging shows that sorting involves exclusion of the receptor proteins from transport carriers destined for the axonal domain at the level of the soma. The neuron-specific glutamate receptor proteins mGluR1, NR2A and NR2B, but not GluR1 and GluR2, are also sorted to the somatodendritic domain by a similar mechanism. Interference with AP-1-dependent somatodendritic sorting causes morphological changes in dendritic spines and decreases the number of synapses. These findings demonstrate that signal-AP-1 interactions mediate

clathrin-dependent sorting of selected transmembrane cargos to the somatodendritic domain of hippocampal neurons. More generally, they support the notion that AP-1 is a global regulator of polarized sorting in different cell types.

RESULTS

Tyrosine-based Signals in the Cytosolic Tails of TfR and CAR Mediate Somatodendritic Sorting

To analyze the mechanisms of somatodendritic sorting in rat hippocampal neurons, we initially used TfR as a model transmembrane protein. TfR is a type II integral membrane protein that functions as an endocytic receptor for iron-loaded transferrin, and that localizes in a polarized manner to the basolateral domain of epithelial cells (Fuller and Simons, 1986) and the somatodendritic domain of neurons (Cameron et al., 1991) by virtue of sorting information contained within its N-terminal cytosolic domain (Figure 1A) (Collawn et al., 1990; Odorizzi and Trowbridge, 1997; West et al., 1997). Confocal fluorescence microscopy of day *in vitro* 10 (DIV10) neurons expressing TfR tagged at its C-terminal ectodomain with monomeric GFP (A206K variant) (TfR-GFP) showed that this protein localized to the dendrites and soma (Figure 1, B and C) but was largely excluded from the axon (Figure 1B, arrowheads, Figure 1C). Quantification of fluorescence intensity in dendrites *vs.* axons in many cells yielded a polarity index of 9.1 ± 3.0 for this protein (Table 1). Thus, the polarized distribution of transgenic TfR-GFP recapitulated that of endogenous TfR (Cameron et al., 1991).

TfR has a cytosolic tail of 67 amino acids comprising an endocytic YXXØ signal (YTRF, residues 20–23) (Figure 1A) (Collawn et al., 1990). Previous deletion analyses showed that several segments of the TfR tail are required for somatodendritic sorting (West et al., 1997), but the exact signals involved were not defined. We performed a mutational analysis of the TfR tail and found that single substitution of alanine for Y20 resulted in loss of polarized distribution of TfR-GFP, with the mutant protein being evenly distributed among the dendrites, soma and axon (Figure 1, B and C) (polarity index: 1.3 ± 0.2; Table 1). Substitution of alanine for F23 also caused appearance of TfR-GFP in the axon (Figure 1, B and C) (polarity index: 1.4 ± 0.2; Table 1). Similar results were obtained with DIV7 neurons transfected with TfR-YFP constructs (Figure S1, A and B). In contrast, mutation of two other phenylalanine residues, F9 or F13 (Figure 1A), had no effect on the somatodendritic localization of TfR-YFP (Figure S1, A and B). We also noticed that whereas wild-type TfR-GFP or TfR-YFP displayed punctate staining in the cytoplasm of dendrites and soma, the corresponding Y20A mutants showed diffuse staining throughout the cell, including the axon (Figure 1, B and C; Figure S2, A–C). The punctate structures containing wild-type TfR-YFP were identified as endosomes by co-localization with internalized antibod y to GFP (which recognizes the YFP tag) (Figure S2, A and B). The diffuse staining of the TfR-YFP Y20A mutant, on the other hand, corresponded to the cell surface, as demonstrated by labeling of non-permeabilized cells at 0°C with the same antibody to GFP (Figure S2C). This change in surface staining is consistent with the known role of Y20 as an element of the YTRF endocytic signal (Collawn et al., 1990). From these experiments we concluded that Y20 and F23 in the TfR tail are components of a somatodendritic sorting signal that overlaps with the YTRF endocytic signal.

We extended our analyses to the type I integral membrane protein, CAR, a cell adhesion molecule that is highly expressed in the developing central nervous system. CAR localizes to the basolateral surface of polarized epithelial cells (Walters et al., 1999; Diaz et al., 2009) by virtue of a cytosolic YXXØ signal, YNQV (resid ues 318–321) (Figure S3A) (Cohen et al., 2001; Carvajal-Gonzalez et al., 2012). We observed that whereas a CAR-GFP construct was restricted to the somatodendritic domain (polarity index: 8.1 ± 1.1), mutants having an

alanine substitution for Y318 or V321 appeared in the axon (polarity index: 1.1 ± 0.2 and 1.2 ± 0.2, respectively) (Figure S3, B and C). Taken together, these experiments demonstrated that tyrosine-based signals fitting the YXXØ consensus motif mediate somatodendritic sorting of two transmembrane cargos, TfR and CAR, in hippocampal neurons.

Interaction of Tyrosine-based Somatodendritic Sorting Signals with the μ1A Subunit of AP-1

Since the epithelial-specific μ1B subunit isoform of AP-1 mediates basolateral sorting in epithelial cells (Folsch et al., 1999; Gan et al., 2002), we hypothesized that the ubiquitous μ1A—the only μ1 isoform that is expressed in the brain (Ohno et al., 1999)—might be responsible for sorting to the somatodendritic domain of neurons. Consistent with this notion, we recently found that μ1A binds to the cytosolic tails of TfR (Gravotta et al., 2012) and CAR (Carvajal-Gonzalez et al., 2012). Further analyses using yeast two-hybrid (Y2H) and *in vitro* binding assays showed that interactions with μ1A require Y20 and F23, but not F9 and F13, in the TfR cytosolic tail (Figure S1, C–E), and Y318 and V321 in the CAR cytosolic tail (Figure S3D) (Carvajal-Gonzalez et al., 2012). These observations demonstrated a strong correlation between the sequence requirements for somatodendritic sorting and for interaction with μ1A, suggesting that both phenomena are functionally linked.

The structural basis for the interaction of YXXØ-type sorting signals with μ1A has not been elucidated. However, X-ray crystallographic studies of the homologous μ2 subunit of AP-2 in complex with YXXØ-containing peptides revealed the presence of a binding site comprising two hydrophobic pockets for the Y and Ø residues (Owen and Evans, 1998). Notably, the residues that line the YXXØ-binding site in μ2, except for K420, are conserved in μ1A, suggesting that this protein has a similar binding site. Indeed, mutation of some of the conserved μ1A residues (*i.e.*, F172, D174, W408 and R410) (Figure 2A) to alanine or serine abrogated interaction with the cytosolic tail of TGN38 (Figure 2B), a TGN-localized, type I transmembrane protein having a prototypical YXXØ motif (YQRL, residues 350–353) (Ohno et al., 1995). Binding of the CAR tail to μ1A exhibited similar requirements (except for R410) (Figure 2B), indicating that the CAR YNQV signal binds to the conserved, canonical site. Surprisingly, binding of the TfR tail to μ1A was only abolished by mutation of W408 (Figure 2B). Thus, although the somatodendritic sorting signals in CAR and TfR both fit the YXXØ motif, the CAR signal binds to a canonical site whereas the TfR signal binds to a different site that only shares a requirement for W408.

Involvement of AP-1 in Somatodendritic Sorting of TfR and CAR

The characterization of the interactions shown in Figure 2B allowed us to devise a dominant-negative approach to test for the involvement of μ1A in somatodendritic sorting. This approach consisted of overexpressing HA-tagged μ1A-wild-type (WT) or μ1A-W408S constructs in hippocampal neurons, and then examining the distribution of TfR-GFP and CAR-GFP in these cells. Both μ1A proteins were equally incorporated into the endogenous AP-1 complex, as determined by immunoprecipitation with antibody to the HA epitope followed by immunoblotting with antibody to the γ-adaptin subunit of AP-1 (Figure 2C). Moreover, confocal fluorescence microscopy showed that both GFP-tagged μ1A-WT and μ1A-W408S co-localized with endogenous γ-adaptin and TGN38 to a juxtanuclear structure typical of the TGN/ RE in the neuronal soma (Figure 2, D and E), as w ell as to dendritic structures previously defined as “Golgi outposts” (Horton et al., 2005) (Figure 2, D and E, diamonds). Co-localization w as extensive, with Manders’ coefficients of ~0.9. Overexpression of μ1A-WT had no effect on the somatodendritic localization of TfR-GFP and CAR-GFP, whereas overexpression of μ1A-W408S resulted in appearance of both

receptors in the axon (Figure 3, A and B; Figure S3E) (polarity indexes shown in Table 1 and Figure S3F). Overall axonal-dendritic polarization and the integrity of the axon initial segment (AIS) were not affected by μ1A-W408S overexpression (Figure S4, A and C). These effects were consistent with the specific requirement of μ1A W408 for signal binding, indicating that signal-recognition by μ1A underlies somatodendritic sorting of TfR and CAR. The involvement of AP-1 in somatodendritic sorting was confirmed by shRNA-mediated knock-down (KD) of γ-adaptin (γ1 isoform) (Kim and Ryan, 2009), which also caused mislocalization of TfR-YFP to axons (Figure S5A). In contrast, shRNA-mediated KD of the μ2 subunit of AP-2 did not lead to axonal missorting of TfR-YFP, even though it redistributed the receptor from endosomes to the plasma membrane (Figure S5B) because of inhibition of endocytosis (Kim and Ryan, 2009).

Dependence of Somatodendritic Sorting on Clathrin

Since AP-1 is a component of clathrin coats associated with the TGN/ RE (Robinson, 2004), we next tested for the involvement clathrin in somatodendritic sorting of TfR. This analysis was performed using dominant-negative interference rather than shRNA-mediated KD because it better preserved the viability of neurons. The basic building block of clathrin coats is the triskelion, a hexameric complex composed of three heavy chains (CHC) and three light chains (CLC). Clathrin function can be perturbed by overexpression of a “hub” fragment comprising the C-terminal third of the CHC (Liu *et al.*, 1998). This construct acts as a dominant-negative inhibitor of clathrin function by competing with endogenous CHC for binding to CLC (Liu et al., 1998). We observed that overexpression of this construct caused mislocalization of TfR-GFP to the axon (Figure 4, A and B) (polarity index: 1.6 ± 0.5; Table 1) without affecting overall dendritic-axonal polarity and the AIS (Figure S4B). Thus, somatodendritic sorting of TfR is also dependent on clathrin.

AP-1-mediated Somatodendritic Sorting Involves Cargo Exclusion from Axonal Carriers at the Level of the Soma

Where in the cell does AP-1 participate in somatodendritic sorting? In principle, AP-1 could act in the soma to exclude somatodendritic cargos from transport carriers bound for the axon (exclusion model). Alternatively, somatodendritic cargos could t ravel to the axon but then be rapidly retrieved to the soma (retrieval model), as previously proposed for transport in *C. elegans* RIA interneurons (Margeta et al., 2009). One criterion to distinguish between these alternative explanations is the intracellular localization of AP-1. As shown in Figure 2 (D and E), both endogenous γ-adaptin and transgenic μ1A localize to the TGN/ RE and dendrites. Moreover, live-cell imaging showed that tubular-vesicular structures decorated with μ1A-GFP moved bi-directionally between the soma and dendrites (Movie S1; Figure 5, A and B), similarly to AP-1-containing, pleiomorphic transport carriers that shuttle between central and peripheral areas of the cytoplasm in non-polarized cell types (Huang et al., 2001; Waguri et al., 2003; Puertollano et al., 2003). These moving structures, however, w ere excluded from the axon, apparently at the level of the AIS (Movie S1; Figure 5, A and B).

Transport carriers containing TfR-YFP also moved in both anterograde and retrograde directions between the soma and dendrites, and to a much lesser extent in the axon (Movie S2), as previously shown (Burack et al., 2000). To assess the role of TfR-tail–AP-1 interactions in this axonal exclusion, we co-expressed TfR-GFP with mCherry-tagged μ1A-WT or μ1A-W408S, together with Tau-CFP to identify axons. Live-cell imaging (Movie S3; Figure 5, C and D) and kymographs (Figure 5, C and D) showed significant increases in the number of TfR-GFP-containing particles moving in anterograde direction (lines with negative slopes in the kymographs) as well as stationary particles (vertical lines in the kymographs) in the axons of cells expressing μ1A-W408S *vs.* μ1A-WT (Figure 5E). The number of retrograde TfR-GFP-containing particles (lines with positive slopes in the

kymographs) was not significantly changed (Figure 5E), although their average intensity increased. Regardless of the conditions, particles moving along the axon exhibited average speeds of 1.0–1.2 μm/ s, characteristic of axonal transport carriers. From these experiments we concluded that disruption of the TfR-tail–AP-1 interaction resulted in misincorporation of TfR into axonal carriers at the level of the TGN/ RE in the neuronal soma.

Requirement of AP-1 for Somatodendritic Sorting of Glutamate Receptor Proteins

To assess whether AP-1 also plays a role in the somatodendritic sorting of neuron-specific proteins, we extended our studies to various glutamate receptors that mediate excitatory synaptic transmission critical for learning and memory (Riedel et al., 2003). These receptors included the mGluR1 metabotropic glutamate receptor 1 (mGluR1), the NR2A and NR2B subunits of NMDA-type and the GluR1 and GluR2 subunits of AMPA-type ionotropic glutamate receptors. Y2H assays showed that portions of the C-terminal cytosolic domains of mGluR1, NR2A and NR2B interacted with μ1A in a manner dependent on μ1A W408 (Figure 6A). We did not attempt the identification of the receptor sequences involved in these interactions because the cytosolic domains are very long relative to those of TfR and CAR. However, the requirement of μ1A W408 for interactions suggests the involvement of YXXØ-type sequences. In line with these binding assays, GFP-tagged forms of mGluR1, NR2A and NR2B localized exclusively to the somatodendritic domain in DIV10 neurons overexpressing μ1A-WT (polarity indexes: 6.3 ± 2.2 to 9.6 ± 2.6; Table 1), but appeared in the axon upon overexpression of μ1A-W408S (polarity indexes: 1.3 ± 0.3 to 1.6 ± 0.4; Table 1) (Figure 6B). In contrast, the cytosolic domains of GluR1 and GluR2 did not exhibit interactions with μ1A in Y2H assays (Figure 6A), and GFP- or SEP-tagged forms of these receptor proteins were restricted to the somatodendritic domain regardless of the overexpression of μ1A-WT (polarity indexes: 8.1 ± 2.0 and 7.0 ± 1.4, respectively; Table 1) or μ1A-W408S (polarity indexes: 7.8 ± 2.0 and 6.9 ± 2.8, respectively; Table 1) (Figure 6B). The exclusive axonal localization of transgenic n euron-glia cell adhesion molecule (NgCAM) (Sampo et al., 2003; Wisco et al., 2003) was unaffected by overexpression of either μ1A-WT (polarity index: 0.1 ± 0.1; Table 1) or μ1A-W408S μ1A-W408S (polarity index: 0.1 ± 0.1; Table 1) (Figure 6B), validating the specificity of the dominant-negative effects for a subset of dendritic proteins. We also examined the effects of μ1A-W408S overexpression on the distribution of several endogenous glutamate receptor proteins in DIV10 neurons. This manipulation also caused missorting of NR2A and NR2B, but not GluR1 and GluR2, to the axon (Figure 7A–D) (Table 1). Taken together, these experiments with transgenic and endogenous forms of glutamate receptor proteins indicated that AP-1 μ1A specifically mediates somatodendritic sorting of selected transmembrane receptors in hippocampal neurons.

Altered Spine Morphology and Decreased Number of Synapses Caused by Disruption of Signal Recognition by μ1A

Many transmembrane receptors are concentrated in dendritic spines and participate in spine morphogenesis and synapse formation (Tada and Sheng, 2006). Having shown that AP-1 controls signal-mediated sorting of at least some of these receptors to the somatodendritic domain, we decided to examine the effects of overexpressing HA-tagged μ1A-WT or μ1A-W408S on spine morphology and synapse formation in more mature, DIV18 neurons. GFP was co-expressed to label the entire volume of the dendrites. Z-stack reconstruction of GFP images showed that overexpression of HA-tagged μ1A-W408S caused a slight decrease in the density of dendritic protrusions (Figure 8, A and B). More significantly, HA-tagged μ1A-W408S resulted in dramatic decreases in the proportion of dendritic protrusions with visible spine heads (Figure 8A) and in staining for the excitatory postsynaptic marker PSD-95 (Figure 8, C and D), both indicative of impaired dendritic spine maturation . In addition, we observed that overexpression of HA-tagged μ1A-W408S decreased the density

of postsynaptic PSD-95 clusters that were juxtaposed to presynaptic synapsin-1 clusters (Figure 8, C and E), a measure of synaptic contacts. Taken together, these experiments revealed a critical requirement of μ1A for dendritic spine maturation and synaptic contacts, which may derive from its function in signal-mediated sorting of specific transmembrane proteins to the somatodendritic domain.

DISCUSSION

The results of our study demonstrate that physical interactions between YXXØ-type, tyrosine-based signals and the μ1A subunit of AP-1 mediate polarized sorting of TfR and CAR to the somatodendritic domain of rat hippocampal neurons. Although characterized in less detail, similar interactions appear to mediate somatodendritic sorting of at least three neuron-specific, glutamate receptor proteins: mGluR1, NR2A and NR2B. In line with the role of AP-1 as a clathrin adaptor, clathrin itself is also required for somatodendritic sorting. Signal-mediated, AP-1/ clathrin-dependent somatodendritic sorting involves exclusion of transmembrane cargoes from axonal transport carriers at the TGN/ RE in the neuronal soma. Failure of this sorting mechanism has dramatic consequences for the anatomical and functional organization of neurons, including a change in the structure of dendritic spines and a decrease in the number of synapses.

YXXØ-μ1A Interactions Involved in Somatodendritic Sorting

Previous studies had established that interactions of tyrosine-based signals with the μ subunits of AP-2, AP-3 and AP-4 mediate various cargo sorting events, including rapid internalization from the plasma membrane, transport to lysosomes and melanosomes, and direct delivery from the TGN to endosomes (Bonifacino and Traub, 2003; Robinson, 2004; Burgos et al., 2010). The μ1A subunit of AP-1 was also known to interact with YXXØ-type signals (Ohno et al., 1995), but the functional significance of these interactions remained unclear. Our findings now show that YXXØ-μ1A interactions play a critical role in cargo sorting to the neuronal somatodendritic domain. The YNQV sequence from CAR behaves as a typical YXXØ signal, in that both the Y and V residues are required for somatodendritic sorting as well as interaction with μ1A (Figure S3) (Carvajal-Gonzalez et al., 2012). Furthermore, this sequence binds to a site on μ1A that is similar to the structurally-defined YXXØ-binding site on μ2 (Figure 2) (Owen and Evans, 1998). The YTRF sequence from TfR also fits the canonical YXXØ motif, and both the Y and F residues are necessary for somatodendritic sorting (Figure 1) and μ1A binding (Figure S1). However, this sequence seems to bind to a different site on μ1A that only shares W408 with the conserved site (Figure 2). This observation points to a potentially new mode of signal recognition by μ subunits.

Our findings highlight both similarities and differences in the mechanisms of somatodendritic sorting in neurons and basolateral sorting in epithelial cells. Among the similarities, interactions of signals with the μ1 subunit of AP-1 underlie both of these polarized sorting events. In addition, the same YXXØ signal in CAR, YNQV, mediates somatodendritic (Figure S3) and basolateral sorting (Cohen 2001); Carvajal-Gonzalez et al., 2012). In the case of TfR, however, basolateral sorting does not depend on the YXXØ signal, YTRF, but on a non-canonical sequence, GDNS (residues 31–34) (Odorizzi and Trowbridge, 1997). We found that mutation of the GDNS sequence has no effect on somatodendritic sorting of TfR (data not shown), in agreement with results from a previous deletion analysis (West et al., 1997). Another key difference is that basolateral sorting of various cargoes, including TfR and CAR, depends mainly on the epithelial-specific μ1B instead of the ubiquitous μ1A (Folsch et al., 1999; Gravotta et al., 2012; Carvajal-Gonzalez et al., 2012). These variations likely represent adaptations of a basic molecular recognition event to the need for achieving polarized sorting in cell types with very different structural

and functional organizations. We anticipate that an even greater degree of variability will be uncovered in the future, in light of the diversity of signals that mediate basolateral and somatodendritic sorting, including dileucine and non-canonical signals (Gonzalez and Rodriguez-Boulan, 2009; Lasiecka and Winckler, 2011), and the existence of multiple AP-1 complexes (*i.e.*, at least 10) resulting from combinatorial assembly of different subunit isoforms (Mattera et al., 2011). In this regard, the failure of μ1A-W408S overexpression to missort the AMPA receptor proteins GluR1 and GluR2 to the axon could be due to the use of a different type of signal or adaptor for somatodendritic sorting. Indeed, somatodendritic sorting of AMPA receptors was recently shown to occur through association with transmembrane AMPA receptor regulatory proteins (TARPs), which in turn interact with the AP-4 complex (Matsuda et al., 2008).

Somatodendritic Sorting Involves Exclusion of Cargo Proteins from Axonal Carriers at the TGN/RE

Recognition of somatodendritic sorting signals by AP-1 causes exclusion of TfR from axonal transport carriers at the TGN/ RE within the neuronal soma. This conclusion is predicated on the predominant localization of AP-1 to the soma and dendrites, and its depletion from the axon (Figures 2 and 5; Movie S1). Moreover, TfR-containing transport carriers emanating from the juxtanuclear cytoplasm move freely into the dendrites but are prevented from entering the axon at the level of the AIS (Movie S2) (Burack et al., 2000). Evidently, these dendritic transport carriers lack the means (*e.g.*, some specific motor molecule) to traverse the filter imposed by the AIS (Song et al., 2009). AP-1 has been shown to interact with kinesin-1 (Schmidt et al., 2009) and kinesin-3 (Nakagawa et al., 2000) family members, but the roles of these interactions in dendritic transport remain to be examined. Our results do not exclude the occurrence of small amounts of AP-1 and TfR in the axon, but clearly indicate that this is not their prevalent localization. Disruption of the signal–AP-1 interaction results in incorporation of TfR into axonal carriers (Figure 5). This allows TfR to overcome the AIS barrier and travel along the axon on a different type of carrier. Significantly, disruption of the signal–AP-1 interaction does not re-route all the TfR into axons, nor does it prevent TfR incorporation into dendritic carriers; it just leads to its non-polarized transport and distribution throughout the neuron (Figures 1 and 3). These observations underscore an important concept concerning the role of signal-adaptor interactions in polarized sorting in both neurons and epithelial cells: somatodendritic and basolateral sorting signals are often not required to enable transport into these domains but to prevent transport into the axonal and apical domains, respectively.

At least two models can be entertained to explain how AP-1 prevents cargo incorporation into axonal transport carriers. One model is that AP-1, in conjunction with clathrin, sequesters cargo away from regions of the TGN/ RE where axonal carriers form. This could involve segregation into a clathrin-coated domain on the source organelle or formation of a population of clathrin-coated carriers that mediate transport to the somatodendritic domain. An alternative model is tha t AP-1/ clathrin-coated intermediates remove somatodendritic proteins from axonal carrier precursors and return them to the TGN/ RE, in a manner analogous to the retrieval of mannose 6-phosphate receptors and their lysosomal enzyme ligands from immature secretory granules (Klumperman et al., 1998). Exactly which of these models explains axonal exclusion will have to be determined by higher resolution analyses of AP-1 localization and dynamics in relation to those of cargo proteins.

AP-1 as a Global Regulator of Polarized Sorting

The role of signal-AP-1 interactions in somatodendritic sorting is not limited to hippocampal neurons but is also observed it in cortical neurons (G. Farías, unpublished observations). Moreover, this basic role appears to be evolutionarily conserved. Indeed, studies in *C.*

elegans have shown that the μ1 ortholog UNC-101 is required for sorting of transmembrane proteins such as the odorant receptor ODR-10 (Dwyer et al., 2001; Kaplan et al., 2010) and the polycystin 2 channel TRPP2 (Bae et al., 2006) to olfactory cilia, a specialized dendritic subdomain of chemosensory neurons. *C. elegans* UNC-101 also plays a role in the sorting of several postsynaptic receptors to dendrites of RIA interneurons (Margeta et al., 2009). Despite this conservation, there are important differences in the way that UNC-101/ μ1A promotes dendritic sorting in *C. elegans* and mammalian neurons. In chemosensory neurons from *unc-101* mutant worms, ODR-10 is completely absent from both anterograde and retrograde dendritic vesicles (Dwyer et al., 2001), in contrast to μ1A-deficient rat hippocampal neurons, in which dendritic transport in both directions is not affected. More strikingly, in RIA interneurons UNC-101 localizes predominantly to the axonal compartment, suggesting a transcytotic mechanism in which post-synaptic receptors are not prevented from entering the axonal compartment but are efficiently retrieved to the soma for eventual delivery to dendrites (Margeta et al., 2009). This is clearly distinct from rat hippocampal neurons wherein μ1A is depleted from axons and functions to prevent transport of somatodendritic proteins to the axon (Figure 5). These differences could be cargo-specific or due to the different anatomical organization of rat hippocampal neurons and *C. elegans* chemosensory and RIA neurons. Indeed, chemosensory neurons are bipolar cells, with a single dendrite that ends in a sensory cilium (Dwyer et al., 2001), and RIA interneurons are pseudounipolar, with a single neurite that bifurcates into an axon and a dendrite (Margeta et al., 2009).

In addition to its role in epithelial cells and neurons, AP-1 is required for Nak-dependent localization of the Dlg protein to the basolateral surface of distal cells of Drosophila salivary glands (Peng et al., 2009), and for preventing the Notch activator Sanpodo from recycling from endosomes to adherens junctions in Drosophila sensory organ precursor cells (Benhra et al., 2011). These examples point to a broad role of AP-1 in the regulation of polarized sorting in various cell types. Although AP-1 has been ascribed many other roles, particularly in transport between the TGN and endosomes in undifferentiated cells and unicellular organisms (Robinson, 2004), mounting evidence indicates that this protein complex functions as a regulator of polarized sorting in differentiated cells and multicellular organisms.

Altered Polarized Sorting May Underlie Neurodevelopmental Disorders Caused by AP-1 Defects

Consistent with the critical role of AP-1 in polarized sorting in many cell types, null mutations in AP-1 subunit genes often cause embryonic lethality in multicellular organisms such as *C. elegans* (Shim et al., 2000), zebrafish (Zizioli et al., 2010) and mouse (Zizioli et al., 1999; Meyer et al., 2000). This is in contrast to the viability of AP-1-null mutant yeast (Phan et al., 1994), Dictyostelium (Lefkir et al., 2003) and mouse embryonic fibroblasts (Meyer et al., 2000) grown in single-cell cultures. Mutations in AP-1 subunit genes also cause two human developmental disorders, the MEDNIK syndrome and a form of X-linked mental retardation (XLMR) that is also referred to as Fried syndrome.

MEDNIK syndrome is a neurocutaneous disorder caused by mutation of the gene encoding σ1A (Montpetit et al., 2008), one of three isoforms of the σ1 subunit of AP-1 (*i.e.*, σ1A, σ1B and σ1C) (Boehm and Bonifacino, 2001; Mattera et al., 2011). Fried syndrome is a neurodevelopmental disorder that results from mutations in σ1B (Tarpey et al., 2006). Both disorders present with mental retardation and a range of other anatomical and functional abnormalities of the central nervous system. It is currently unclear how deficiency of a σ1 isoform could cause these diseases. One possibility is that σ1 isoforms are differentially expressed in different cell populations. Alternatively, σ1 isoforms could endow AP-1 with different cargo-recognition specificities, as recently shown for the binding of proteins with

dileucine-based sorting signals (Mattera et al., 2011). In either case, our findings suggest that these disorders may arise from failure to sort certain cargos to the somatodendritic domain of specific neuron al populations.

EXPERIMENTAL PROCEDURES

Cell Culture and Transfection

Primary cultures of rat hippocampal neurons were prepared as previously described (Caceres et al., 1984). Briefly, hippocampi were dissected from Sprague-Dawley rats on embryonic day 18, and dissociated with trypsin. Cells were plated onto poly-L-lysine-treated plates and maintained in DMEM supplemented with 10% v/v horse serum for 2–3 h. The culture medium was then substituted with Neurobasal medium supplemented with B-27 and Glutamax (Invitrogen). After 3–4 days in culture, neurons were transfected with different plasmid constructs (see Supplemental Experimental Procedures) using Lipofectamine 2000 (Invitrogen), except for biochemical studies where nucleofection was performed in suspension using the Amaxa system (Lonza). Neurons were analyzed after different times in culture (indicated in legends to figures), in most cases at DIV10 for analyses of polarized sorting and DIV18 for analyses of dendritic spine and synapses. In all neurons, the dendrites and AIS were identified by immunostaining with antibodies to MAP2 and Ank-G, respectively.

Fluorescence Microscopy and Image Analysis

Neurons expressing different transgenic proteins were fixed, permeabilized, and stained with primary antibodies (see Supplemental Experimental Procedures) followed by appropriate fluorescently-labeled secondary antibodies (Molecular Probes, Invitrogen). Fluorescence images were obtained using a confocal microscope (LSM710, Zeiss) fitted with a 63X, 1.4 NA objective. Image analysis was performed using Image J version 1.44o (Wayne Rasband, N IH; http:/ / imagej.nih.gov). For each condition, 7–14 cells from 3 different cultures were analyzed. The polarity index was calculated as previously described (Sampo et al., 2003; Wisco et al., 2003). Briefly, several one-pixel lines were traced along 3 dendrites and representative portions of the axon using MAP2, tubulin-mCherry or GFP as guides. An average Dendrite:Axon (D:A) ratio was calculated for each cell (D:A=1, uniform staining; D:A<1, preferential axonal staining; D:A>1, preferential dendritic staining). To calculate the density of dendritic protrusions, neurons co-expressing GFP and HA-tagged μ1A-WT or μ1A-W408 mutant were immunostained for PSD-95 (postsynaptic marker) and synapsin-1 (presynaptic marker). The numbers of protrusions below 3 μm in length with visible spine heads, PSD-95 positive protrusions, and presynaptic-postsynaptic contacts were counted. Synaptic cluster parameters were determined as previously described (Farias et al., 2009).

Live-cell Imaging

Live neurons expressing fluorescently-tagged proteins were imaged on a spinning-disk microscope (Marianas, Intelligent Imaging) equipped with 63X, 1.4 NA or 100X, 1.4 NA objectives. Digital images were acquired with an EM-CCD camera (Evolve, Photometrics). TfR-GFP imaging in neurons expressing μ1A-mCherry (WT or W408 mutant) involved 200 ms exposures and recording every 250 ms for 30–60 s. For μ1A-GFP imaging, 200 ms exposure and recording every 5 s for 600 s was used. Three transfected neurons from each coverslip were chosen for time-lapse imaging from 6–8 independent experiments, and a single level of focus was maintained throughout each recording. Axons were identified morphologically by their length and thin diameter, and by co-expression of Tau-CFP. Image processing and analysis was performed using Image J as detailed in Supplemental Experimental Procedures.

Yeast Two-hybrid (Y2H) Analysis

Complementary DNAs encoding cytosolic tail sequences from human TfR (residues 1–67), human CAR isoform 1 (261–365), rat mGluR1 isoform a (841–1199), human NR2A (1304–1464), human NR2B (1315–1484), human GluR1 (827–906) and rat GluR2 (834–883) were amplified by PCR and cloned into the Gal4 binding domain (BD) vectors pGBKT7 or pGBT9 (Clontech). Full-length mouse μ1A was cloned in the Gal4 activation domain (AD) vector pACT2 (Clontech). Transformation of the AH109 yeast reporter strain with BD- and AD-vectors, and plate selection was performed as previously described (Mattera et al., 2003).

Additional Methods

Additional information on DNA constructs, Y2H analysis, GST pull-downs, immunofluorescence microscopy, immunoprecipitation, antibodies and statistical analysis is provided in Supplemental Experimental Procedures.

Supplementary Material

Refer to Web version on PubMed Central for supplementary material.

Acknowledgments

We thank X. Zhu and N. Tsai for expert technical assistance, D. Arnold, G. Bloom, F. Brodsky, E. Gundelfinger, K. Howell, P. Kammermeier, J. Lippincott-Schwartz, G. Mardones, M. Nonet, M. Parsons, T. Ryan, L. Traub, S. Vicini and B. Winckler for kind gifts of reagents, and J. Hurley for helpful discussions and critical reading of the manuscript. This work was funded by the Intramural Program of NICHD, NIH.

REFERENCES

Arimura N, Kaibuchi K. Key regulators in neuronal polarity. Neuron. 2005; 48:881–884. [PubMed: 16364893]

Bae YK, Qin H, Knobel KM, Hu J, Rosenbaum JL, Barr MM. General and cell-type specific mechanisms target TRPP2/PKD-2 to cilia. Development. 2006; 133:3859–3870. [PubMed: 16943275]

Benhra N, Lallet S, Cotton M, Le Bras S, Dussert A, Le Borgne R. AP-1 controls the trafficking of Notch and Sanpodo toward E-cadherin junctions in sensory organ precursors. Curr Biol. 2011; 21:87–95. [PubMed: 21194948]

Boehm M, Bonifacino JS. Adaptins: the final recount. Mol Biol Cell. 2001; 12:2907–2920. [PubMed: 11598180]

Bonifacino JS, Traub LM. Signals for sorting of transmembrane proteins to endosomes and lysosomes. Annu Rev Biochem. 2003; 72:395–447. [PubMed: 12651740]

Burack MA, Silverman MA, Banker G. The role of selective transport in neuronal protein sorting. Neuron. 2000; 26:465–472. [PubMed: 10839364]

Burgos PV, Mardones GA, Rojas AL, daSilva LL, Prabhu Y, Hurley JH, Bonifacino JS. Sorting of the Alzheimer's disease amyloid precursor protein mediated by the AP-4 complex. Dev Cell. 2010; 18:425–436. [PubMed: 20230749]

Caceres A, Banker G, Steward O, Binder L, Payne M. MAP2 is localized to the dendrites of hippocampal neurons which develop in culture. Brain Res. 1984; 315:314–318. [PubMed: 6722593]

Cameron PL, Sudhof TC, Jahn R, De Camilli P. Colocalization of synaptophysin with transferrin receptors: implications for synaptic vesicle biogenesis. J Cell Biol. 1991; 115:151–164. [PubMed: 1918133]

Carvajal-Gonzalez JM, Gravotta D, Mattera R, Diaz F, Bay AP, Roman AC, Schreiner RP, Thuenauer R, Bonifacino JS, Rodriguez-Boulan E. Basolateral sorting of the coxsackie and adenovirus receptor through interaction of a canonical YXXPhi motif with the clathrin adaptors AP-1A and AP-1B. Proc Natl Acad Sci U S A. 2012; 109:3820–3825. [PubMed: 22343291]

Cohen CJ, Gaetz J, Ohman T, Bergelson JM. Multiple regions within the coxsackievirus and adenovirus receptor cytoplasmic domain are required for basolateral sorting. J Biol Chem. 2001; 276:25392–25398. [PubMed: 11316797]

Collawn JF, Stangel M, Kuhn LA, Esekogwu V, Jing SQ, Trowbridge IS, Tainer JA. Transferrin receptor internalization sequence YXRF implicates a tight turn as the structural recognition motif for endocytosis. Cell. 1990; 63:1061–1072. [PubMed: 2257624]

Deborde S, Perret E, Gravotta D, Deora A, Salvarezza S, Schreiner R, Rodriguez-Boulan E. Clathrin is a key regulator of basolateral polarity. Nature. 2008; 452:719–723. [PubMed: 18401403]

Diaz F, Gravotta D, Deora A, Schreiner R, Schoggins J, Falck-Pedersen E, Rodriguez-Boulan E. Clathrin adaptor AP1B controls adenovirus infectivity of epithelial cells. Proc Natl Acad Sci U S A. 2009; 106:11143–11148. [PubMed: 19549835]

Dotti CG, Simons K. Polarized sorting of viral glycoproteins to the axon and dendrites of hippocampal neurons in culture. Cell. 1990; 62:63–72. [PubMed: 2163770]

Dwyer ND, Adler CE, Crump JG, L'Etoile ND, Bargmann CI. Polarized dendritic transport and the AP-1 mu1 clathrin adaptor UNC-101 localize odorant receptors to olfactory cilia. Neuron. 2001; 31:277–287. [PubMed: 11502258]

Farias GG, Alfaro IE, Cerpa W, Grabowski CP, Godoy JA, Bonansco C, Inestrosa NC. Wnt-5a/JNK signaling promotes the clustering of PSD-95 in hippocampal neurons. J Biol Chem. 2009; 284:15857–15866. [PubMed: 19332546]

Folsch H, Ohno H, Bonifacino JS, Mellman I. A novel clathrin adaptor complex mediates basolateral targeting in polarized epithelial cells. Cell. 1999; 99:189–198. [PubMed: 10535737]

Fuller SD, Simons K. Transferrin receptor polarity and recycling accuracy in "tight" and "leaky" strains of Madin-Darby canine kidney cells. J Cell Biol. 1986; 103:1767–1779. [PubMed: 2877994]

Gan Y, McGraw TE, Rodriguez-Boulan E. The epithelial-specific adaptor AP1B mediates post-endocytic recycling to the basolateral membrane. Nat Cell Biol. 2002; 4:605–609. [PubMed: 12105417]

Gonzalez A, Rodriguez-Boulan E. Clathrin and AP1B: key roles in basolateral trafficking through trans-endosomal routes. FEBS Lett. 2009; 583:3784–3795. [PubMed: 19854182]

Gravotta D, Carvajal-Gonzalez JM, Mattera R, Deborde S, Banfelder J, Bonifacino JS, Rodriguez-Boulan E. Novel Role of the Clathrin Adaptor AP-1A in Basolateral Polarity. Dev Cell. 2012 In press,

Heldwein EE, Macia E, Wang J, Yin HL, Kirchhausen T, Harrison SC. Crystal structure of the clathrin adaptor protein 1 core. Proc Natl Acad Sci U S A. 2004; 101:14108–14113. [PubMed: 15377783]

Horton AC, Ehlers MD. Neuronal polarity and trafficking. Neuron. 2003; 40:277–295. [PubMed: 14556709]

Huang F, Nesterov A, Carter RE, Sorkin A. Trafficking of yellow-fluorescent- protein-tagged mu1 subunit of clathrin adaptor AP-1 complex in living cells. Traffic. 2001; 2:345–357. [PubMed: 11350630]

Jareb M, Banker G. The polarized sorting of membrane proteins expressed in cultured hippocampal neurons using viral vectors. Neuron. 1998; 20:855–867. [PubMed: 9620691]

Kaplan OI, Molla-Herman A, Cevik S, Ghossoub R, Kida K, Kimura Y, Jenkins P, Martens JR, Setou M, Benmerah A, Blacque OE. The AP-1 clathrin adaptor facilitates cilium formation and functions with RAB-8 in C. elegans ciliary membrane transport. J Cell Sci. 2010; 123:3966–3977. [PubMed: 20980383]

Kim SH, Ryan TA. Synaptic vesicle recycling at CNS synapses without AP-2. J Neurosci. 2009; 29:3865–3874. [PubMed: 19321783]

Klumperman J, Kuliawat R, Griffith JM, Geuze HJ, Arvan P. Mannose 6-phosphate receptors are sorted from immature secretory granules via adaptor protein AP-1, clathrin, and syntaxin 6-positive vesicles. J Cell Biol. 1998; 141:359- 371. [PubMed: 9548715]

Lasiecka ZM, Winckler B. Mechanisms of polarized membrane trafficking in neurons -- focusing in on endosomes. Mol Cell Neurosci. 2011; 48:278–287. [PubMed: 21762782]

Lefkir Y, de Chassey B, Dubois A, Bogdanovic A, Brady RJ, Destaing O, Bruckert F, O'Halloran TJ, Cosson P, Letourneur F. The AP-1 clathrin-adaptor is required for lysosomal enzymes sorting and

biogenesis of the contractile vacuole complex in Dictyostelium cells. Mol Biol Cell. 2003; 14:1835–1851. [PubMed: 12802059]

Liu SH, Marks MS, Brodsky FM. A dominant-negative clathrin mutant differentially affects trafficking of molecules with distinct sorting motifs in the class II major histocompatibility complex (MHC) pathway. J Cell Biol. 1998; 140:1023–1037. [PubMed: 9490717]

Margeta MA, Wang GJ, Shen K. Clathrin adaptor AP-1 complex excludes multiple postsynaptic receptors from axons in C. elegans. Proc Natl Acad Sci U S A. 2009; 106:1632–1637. [PubMed: 19164532]

Matsuda S, Miura E, Matsuda K, Kakegawa W, Kohda K, Watanabe M, Yuzaki M. Accumulation of AMPA receptors in autophagosomes in neuronal axons lacking adaptor protein AP-4. Neuron. 2008; 57:730–745. [PubMed: 18341993]

Mattera R, Arighi CN, Lodge R, Zerial M, Bonifacino JS. Divalent interaction of the GGAs with the Rabaptin-5-Rabex-5 complex. EMBO J. 2003; 22:78–88. [PubMed: 12505986]

Mattera R, Boehm M, Chaudhuri R, Prabhu Y, Bonifacino JS. Conservation and diversification of dileucine signal recognition by adaptor protein (AP) complex variants. J Biol Chem. 2011; 286:2022–2030. [PubMed: 21097499]

Meyer C, Zizioli D, Lausmann S, Eskelinen EL, Hamann J, Saftig P, von Figura K, Schu P. mu1A-adaptin-deficient mice: lethality, loss of AP-1 binding and rerouting of mannose 6-phosphate receptors. EMBO J. 2000; 19:2193–2203. [PubMed: 10811610]

Montpetit A, Cote S, Brustein E, Drouin CA, Lapointe L, Boudreau M, Meloche C, Drouin R, Hudson TJ, Drapeau P, Cossette P. Disruption of AP1S1, causing a novel neurocutaneous syndrome, perturbs development of the skin and spinal cord. PLoS Genet. 2008; 4:e1000296. [PubMed: 19057675]

Nakagawa T, Setou M, Seog D, Ogasawara K, Dohmae N, Takio K, Hirokawa N. A novel motor, KIF13A, transports mannose-6-phosphate receptor to plasma membrane through direct interaction with AP-1 complex. Cell. 2000; 103:569–581. [PubMed: 11106728]

Odorizzi G, Trowbridge IS. Structural requirements for basolateral sorting of the human transferrin receptor in the biosynthetic and endocytic pathways of Madin-Darby canine kidney cells. J Cell Biol. 1997; 137:1255–1264. [PubMed: 9182660]

Ohno H, Stewart J, Fournier MC, Bosshart H, Rhee I, Miyatake S, Saito T, Gallusser A, Kirchhausen T, Bonifacino JS. Interaction of tyrosine-based sorting signals with clathrin-associated proteins. Science. 1995; 269:1872–1875. [PubMed: 7569928]

Ohno H, Tomemori T, Nakatsu F, Okazaki Y, Aguilar RC, Foelsch H, Mellman I, Saito T, Shirasawa T, Bonifacino JS. Mu1B, a novel adaptor medium chain expressed in polarized epithelial cells. FEBS Lett. 1999; 449:215–220. [PubMed: 10338135]

Owen DJ, Evans PR. A structural explanation for the recognition of tyrosine-based endocytotic signals. Science. 1998; 282:1327–1332. [PubMed: 9812899]

Peng YH, Yang WK, Lin WH, Lai TT, Chien CT. Nak regulates Dlg basal localization in Drosophila salivary gland cells. Biochem Biophys Res Commun. 2009; 382:108–113. [PubMed: 19258011]

Phan HL, Finlay JA, Chu DS, Tan PK, Kirchhausen T, Payne GS. The Saccharomyces cerevisiae APS1 gene encodes a homolog of the small subunit of the mammalian clathrin AP-1 complex: evidence for functional interaction with clathrin at the Golgi complex. EMBO J. 1994; 13:1706–1717. [PubMed: 8157009]

Puertollano R, van der Wel NN, Greene LE, Eisenberg E, Peters PJ, Bonifacino JS. Morphology and dynamics of clathrin/GGA1-coated carriers budding from the trans-Golgi network. Mol Biol Cell. 2003; 14:1545–1557. [PubMed: 12686608]

Riedel G, Platt B, Micheau J. Glutamate receptor function in learning and memory. Behav Brain Res. 2003; 140:1–47. [PubMed: 12644276]

Robinson MS. Adaptable adaptors for coated vesicles. Trends Cell Biol. 2004; 14:167–174. [PubMed: 15066634]

Sampo B, Kaech S, Kunz S, Banker G. Two distinct mechanisms target membrane proteins to the axonal surface. Neuron. 2003; 37:611–624. [PubMed: 12597859]

Schmidt MR, Maritzen T, Kukhtina V, Higman VA, Doglio L, Barak NN, Strauss H, Oschkinat H, Dotti CG, Haucke V. Regulation of endosomal membrane traffic by a Gadkin/AP-1/kinesin KIF5 complex. Proc Natl Acad Sci U S A. 2009; 106:15344–15349. [PubMed: 19706427]

Shim J, Sternberg PW, Lee J. Distinct and redundant functions of mu1 medium chains of the AP-1 clathrin-associated protein complex in the nematode Caenorhabditis elegans. Mol Biol Cell. 2000; 11:2743–2756. [PubMed: 10930467]

Silverman MA, Peck R, Glover G, He C, Carlin C, Banker G. Motifs that mediate dendritic targeting in hippocampal neurons: a comparison with basolateral targeting signals. Mol Cell Neurosci. 2005; 29:173–180. [PubMed: 15911342]

Song AH, Wang D, Chen G, Li Y, Luo J, Duan S, Poo MM. A selective filter for cytoplasmic transport at the axon initial segment. Cell. 2009; 136:1148–1160. [PubMed: 19268344]

Tada T, Sheng M. Molecular mechanisms of dendritic spine morphogenesis. Curr Opin Neurobiol. 2006; 16:95–101. [PubMed: 16361095]

Tarpey PS, Stevens C, Teague J, Edkins S, O'Meara S, Avis T, Barthorpe S, Buck G, Butler A, Cole J, Dicks E, Gray K, Halliday K, Harrison R, Hills K, Hinton J, Jones D, Menzies A, Mironenko T, Perry J, Raine K, Richardson D, Shepherd R, Small A, Tofts C, Varian J, West S, Widaa S, Yates A, Catford R, Butler J, Mallya U, Moon J, Luo Y, Dorkins H, Thompson D, Easton DF, Wooster R, Bobrow M, Carpenter N, Simensen RJ, Schwartz CE, Stevenson RE, Turner G, Partington M, Gecz J, Stratton MR, Futreal PA, Raymond FL. Mutations in the gene encoding the Sigma 2 subunit of the adaptor protein 1 complex, AP1S2, cause X-linked mental retardation. Am J Hum Genet. 2006; 79:1119–1124. [PubMed: 17186471]

Waguri S, Dewitte F, Le Borgne R, Rouille Y, Uchiyama Y, Dubremetz JF, Hoflack B. Visualization of TGN to endosome trafficking through fluorescently labeled MPR and AP-1 in living cells. Mol Biol Cell. 2003; 14:142–155. [PubMed: 12529433]

Walters RW, Grunst T, Bergelson JM, Finberg RW, Welsh MJ, Zabner J. Basolateral localization of fiber receptors limits adenovirus infection from the apical surface of airway epithelia. J Biol Chem. 1999; 274:10219–10226. [PubMed: 10187807]

West AE, Neve RL, Buckley KM. Identification of a somatodendritic targeting signal in the cytoplasmic domain of the transferrin receptor. J Neurosci. 1997; 17:6038–6047. [PubMed: 9236215]

Wisco D, Anderson ED, Chang MC, Norden C, Boiko T, Folsch H, Winckler B. Uncovering multiple axonal targeting pathways in hippocampal neurons. J Cell Biol. 2003; 162:1317–1328. [PubMed: 14517209]

Zizioli D, Forlanelli E, Guarienti M, Nicoli S, Fanzani A, Bresciani R, Borsani G, Preti A, Cotelli F, Schu P. Characterization of the AP-1 mu1A and mu1B adaptins in zebrafish (Danio rerio). Dev Dyn. 2010; 239:2404–2412. [PubMed: 20652956]

Zizioli D, Meyer C, Guhde G, Saftig P, von Figura K, Schu P. Early embryonic death of mice deficient in gamma-adaptin. J Biol Chem. 1999; 274:5385–5390. [PubMed: 10026148]

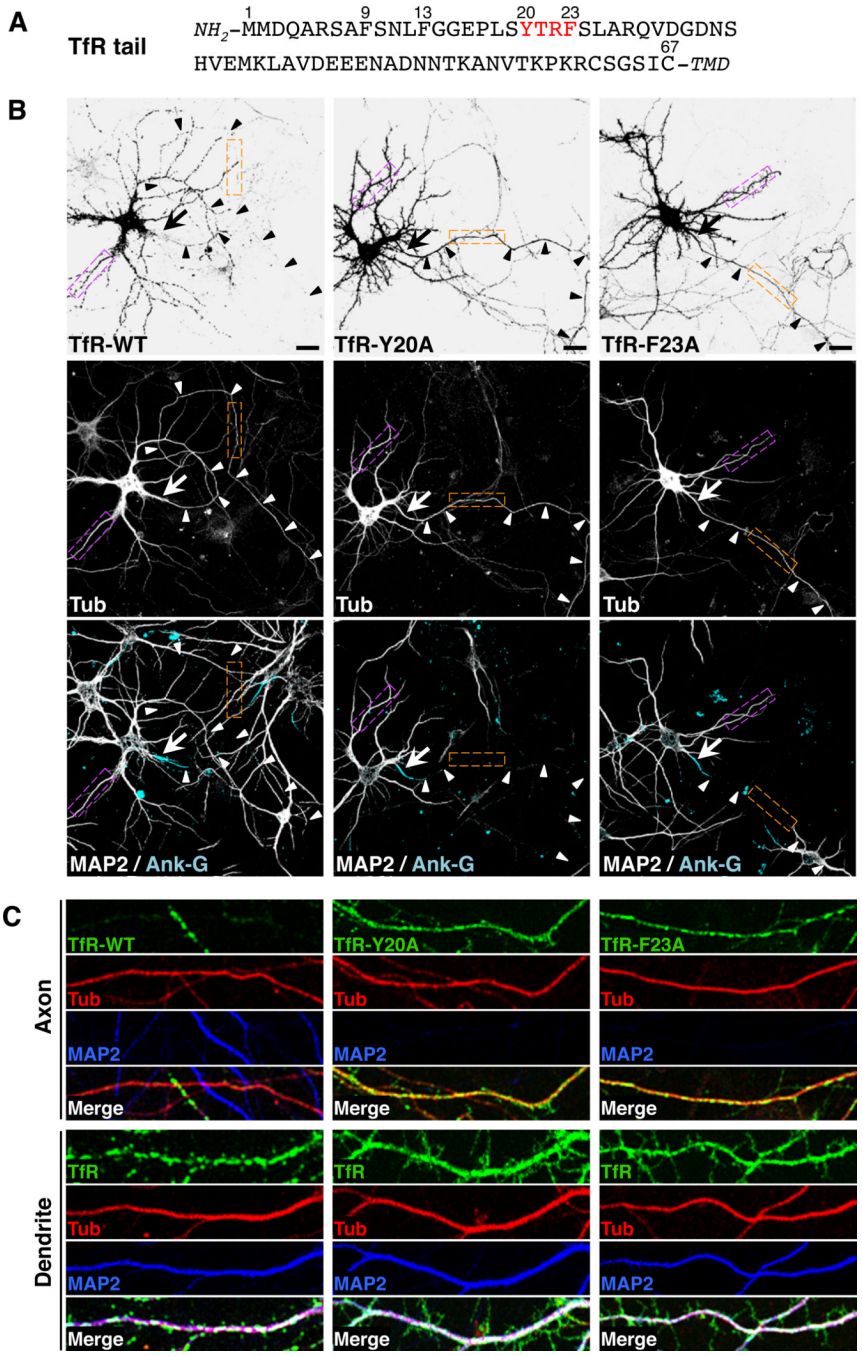

Figure 1. A tyrosine-based motif in the cytosolic tail of TfR is required for its somatodendritic sorting

(A) Amino-acid sequence of the TfR tail indicating residue numbers and a tyrosine-based YXXØ motif (red). TMD: transmembrane domain.

(B) Neurons (DIV10) expressing monomeric-GFP-tagged TfR-WT, TfR-Y20A or TfRF23A (grayscale negative, top panels) and mCherry-tagged tubulin (Tub, grayscale, middle panels) were double-immunostained for MAP2 (grayscale, bottom panels) and ankyrin G (Ank-G, cyan, bottom panels). In this figure as well as other figures, MAP2 was used as a marker for dendrites and Ank-G as a marker for the axon initial segment (AIS). mCherry-tagged tubulin

was a marker for both dendrites and axons. Arrows point to the AIS and arrowheads indicate the axon in each neuron. Scale bars: 20 μm.

(C) Images of axons (top panels) and dendrites (bottom panels) magnified 5X from orange and magenta boxes, respectively, in *B*. TfR-GFP (green), mCherry-tubulin (red), MAP2 (blue), and merged images are shown. White and yellow in the merged images indicate co-localization. Experiments testing the effects of several amino acid substitutions in the TfR cytosolic tail on the polarized distribution of TfR-YFP and interactions of the TfR cytosolic tail with the μ1A subunit of AP-1 and with the AP-1 core are shown in Figure S1. Surface staining and internalization of YFP-tagged TfR-WT and TfR-Y20A are shown in Figure S2. The effects of amino acid substitutions in the cytosolic tail of CAR on the polarized distribution of GFP-tagged CAR in neurons and on its interaction with the μ1A subunit of AP-1 are shown in Figure S3.

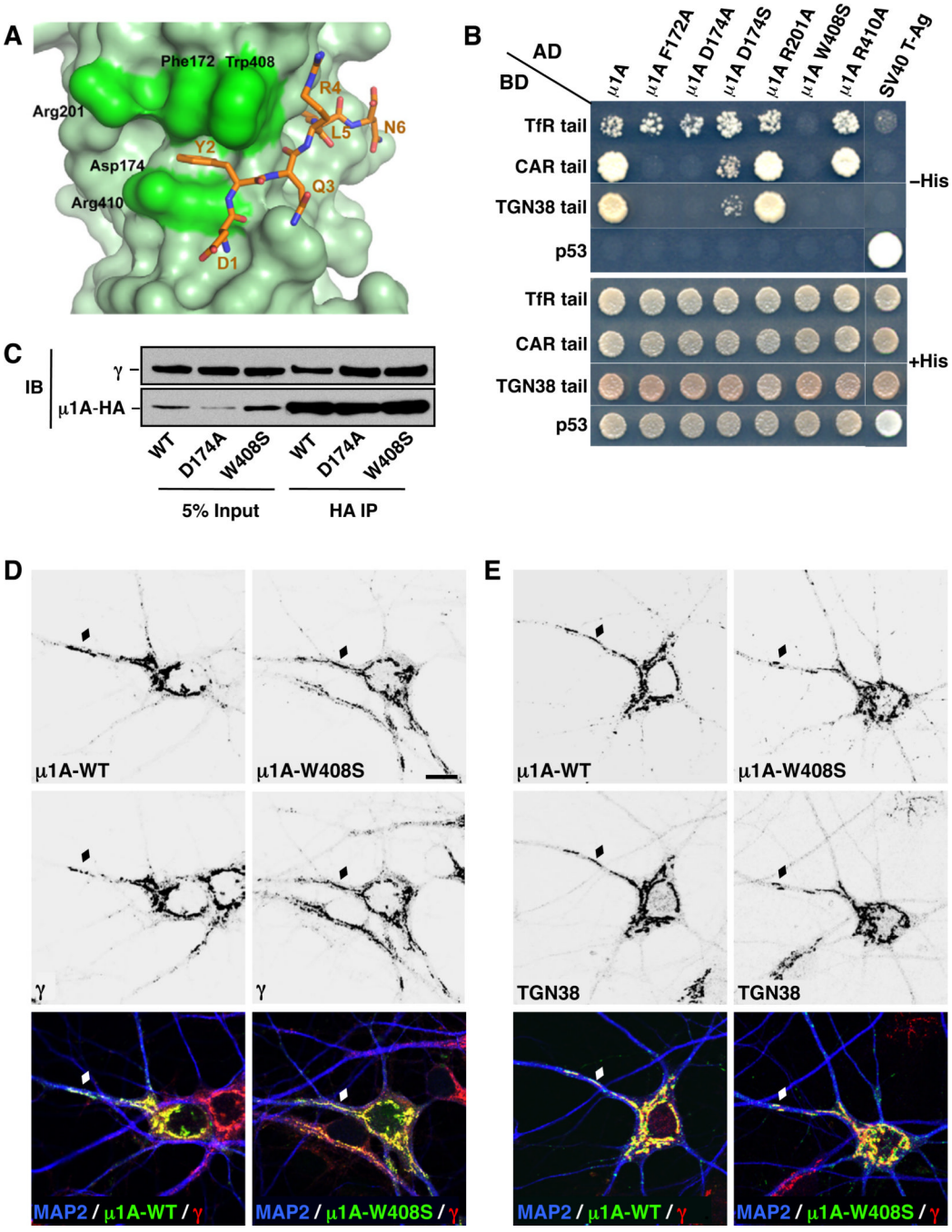

Figure 2. Identification of residues on μ1A that are critical for interactions with tyrosine-based motifs in the cytosolic tails of TfR and CAR

(A) Surface representation of the C-terminal domain of mouse μ1A (light green) (PDB id: 1W63, Heldwein et al., 2004) with ball and stick representation of the DYQRLN peptide from TGN38 (brown) modeled after the structure of the C-terminal domain of rat μ2 in complex with this peptide (PDB id: 1BXX, Owen and Evans, 1998). Residues targeted by mutagenesis are highlighted in green. Model built with PyMOL (DeLano, W.L. The PyMOL Molecular Graphics System (2002) DeLano Scientific, San Carlos, CA).

(B) Y2H analysis of the interaction of the cytosolic tails of TfR (residues 1–67), CAR (residues 261–365) or TGN38 (residues 324–353) with WT and mutant forms of μ1A.

Growth on plates lacking histidine (-His) is indicative of interactions. Co-transformations of cytosolic tail constructs with SV40 T-Ag, and of μ1A constructs with p53, w ere used as negative controls, and p53-SV40 T-Ag co-transformation was used as a positive control. Results are representative of three experiment s with similar results.

(C) Extracts from neurons (DIV-7) expressing transgenic HA-epitope-tagged μ1A-WT, μ1A-D174A or μ1A-W408S were subjected to immunoprecipitation (IP) with antibody to the HA epitope followed by immunoblotting (IB) with antibody to the HA epitope or to the γ-adaptin subunit of AP-1. Five percent of the input extract was run alongside for comparison.

(D, E) Immunofluorescence microscopy of neurons (DIV10) expressing transgenic GFP-tagged μ1A-WT or μ1A-W408S (top panels) immunostained for endogenous γ-adaptin (*D*), TGN38 (*E*) (middle panels) and MAP2 (bottom panels, blue). Merged images are shown in the bottom panels. Yellow and white in the merged images indicate co-localization. Diamonds indicate dendritic Golgi outposts. Scale bar: 10 μm.

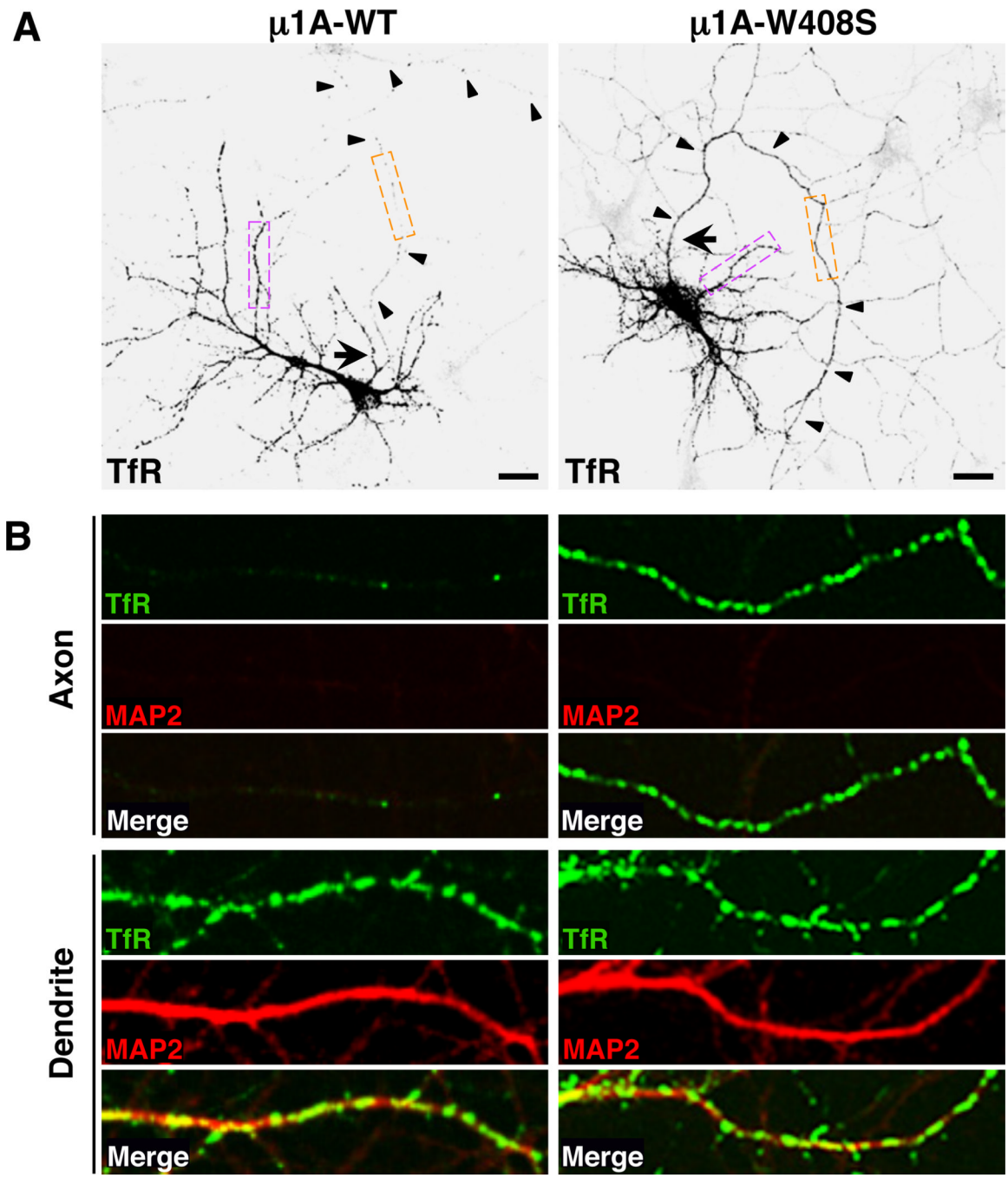

Figure 3. Recognition of a tyrosine-based motif in the TfR tail by μ1A is required for somatodendritic sorting of TfR

(A) Neurons (DIV10) co-expressing transgenic GFP-tagged TfR-WT (grayscale negative, top panels) and HA-tagged μ1A-WT or μ1A-W408S were immunostained for the HA epitope, MAP2 and Ank-G. GFP fluorescence is shown in these panels and the corresponding immunostaining for HA, MAP2 and Ank-G is shown in Figure S4A. Arrow points to the AIS and arrowheads indicate the axon in each neuron. Scale bars: 20 μm. (B) Images of axons (top panels) and dendrites (bottom panels) magnified 5X from orange and magenta boxes, respectively, in *A*. TfR-GFP (green), MAP2 (red), and merged images are shown. Yellow in the merged images indicates co-localization. Similar experiments for

CAR-GFP are shown in Figure S3E. The effects of AP-1 and AP-2 subunits knock-down on the polarized distribution of TfR-YFP are shown in Figure S5.

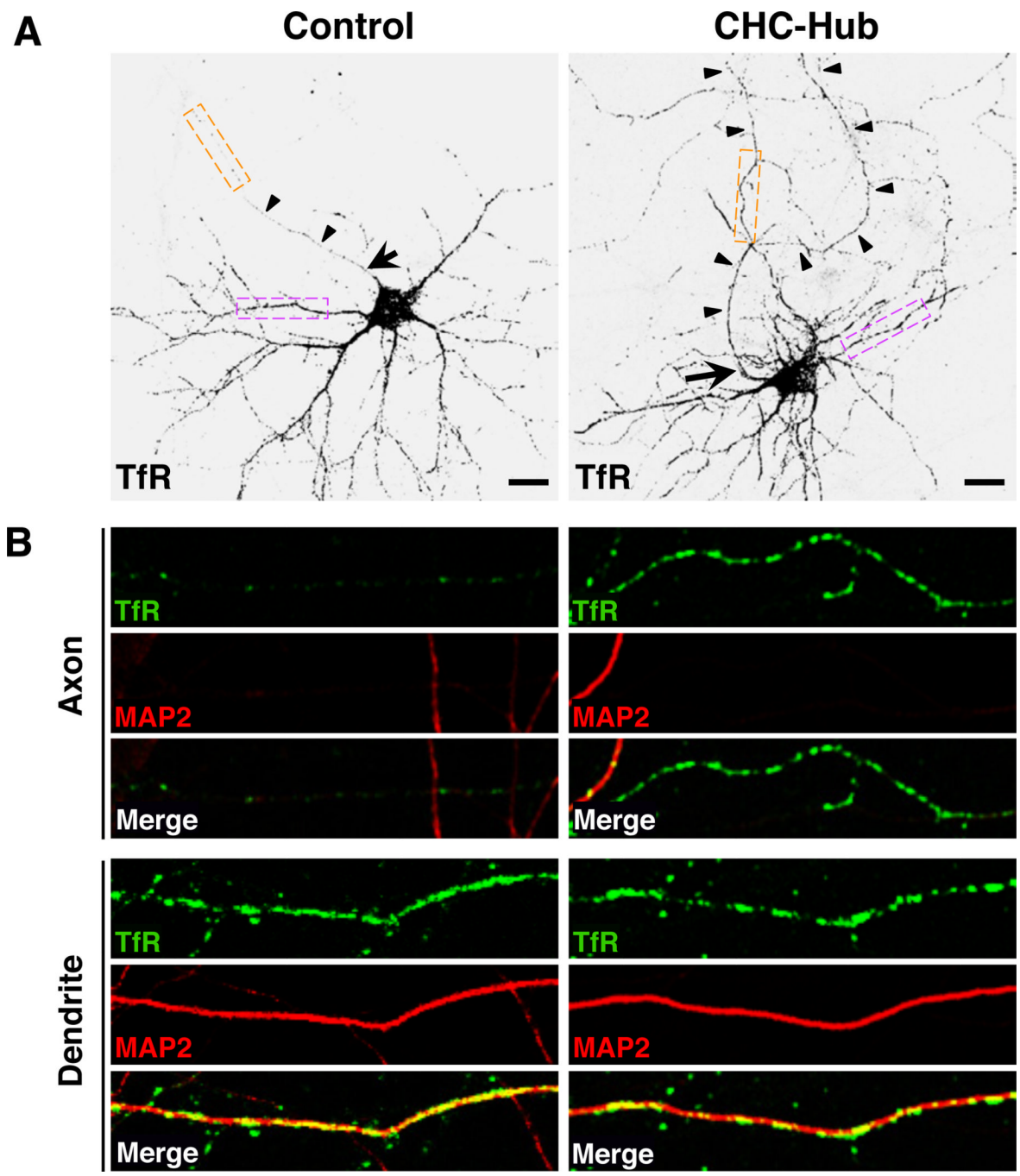

Figure 4. Clathrin is required for somatodendritic sorting of TfR

(A) Neurons (DIV10) co-transfected with plasmids encoding GFP-tagged TfR-WT (grayscale negative, top panels) together with empty vector (control) or vector encoding T7-epitope-tagged clathrin heavy chain hub were immunostained for the T7 epitope, MAP2 and Ank-G. GFP fluorescence is shown in these panels and the corresponding immunostaining for T7, MAP2 and Ank-G is shown in Figure S4B. Arrow points to AIS and arrowheads indicate the axon in each neuron. Scale bars: 20 μm.

(B) Images of axons (top panels) and dendrites (bottom panels) magnified 5X from orange and magenta boxes, respectively, in *A*. TfR-GFP (green), MAP2 (red), and merged images are shown. Yellow in the merged images indicates co-localization.

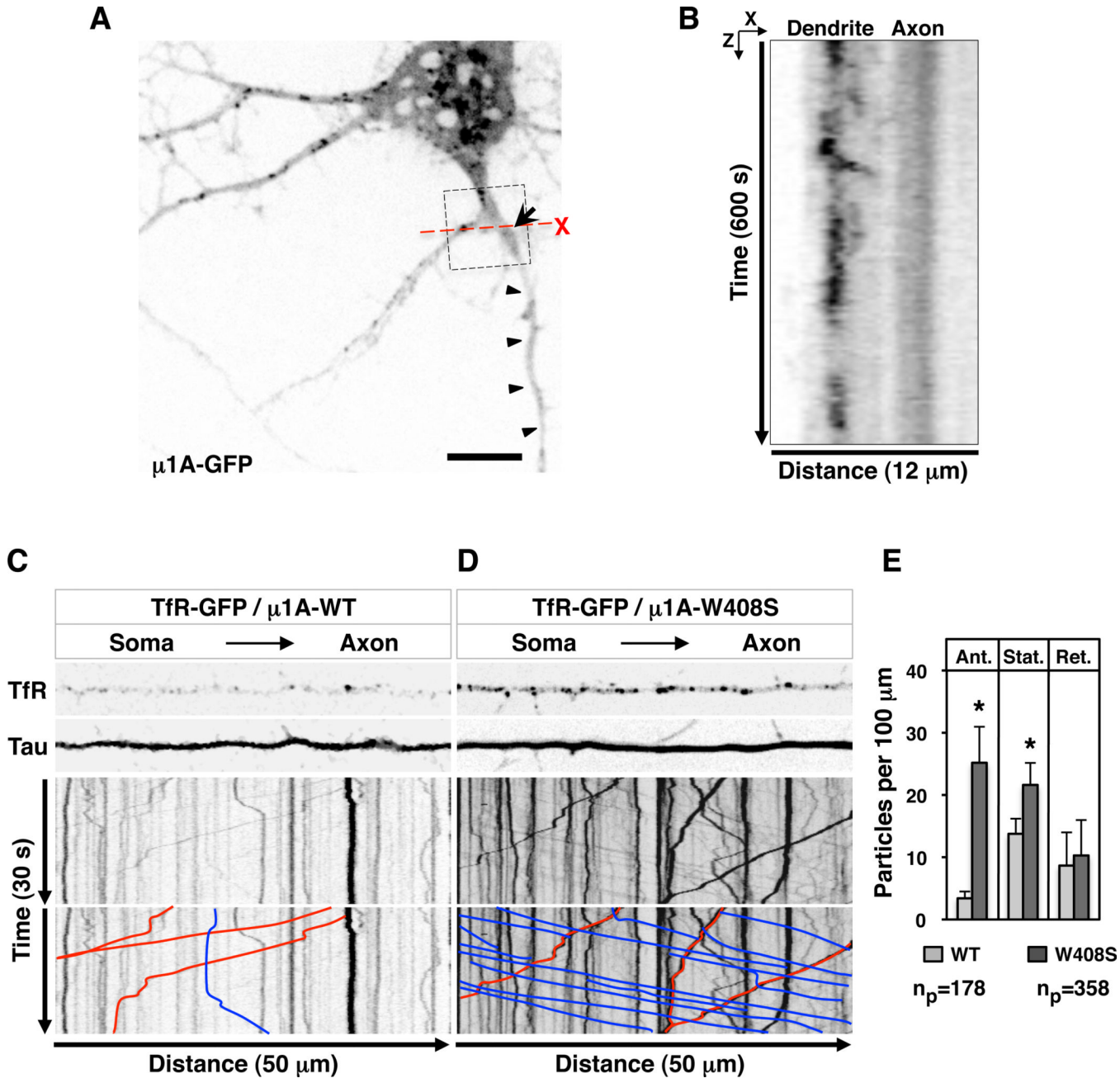

Figure 5. AP-1-mediated somatodendritic sorting of TfR involves exclusion from axonal carriers at the level of the soma

(A) Still image of a neuron (DIV8) expressing transgenic GFP-tagged μ1A (grayscale) taken from time-lapse, live-cell imaging shown in Movie S1. Arrow points to the AIS and arrowheads indicate the axon. Box highlights a bifurcation to a dendrite (left) and an axon (right). Scale bar: 10 μm.

(B) Orthogonal analysis from box in *A* (X plane crossing the proximal segment of dendrite and axon, and Z corresponding to 600 s of recording) shows μ1A-GFP-containing particles crossing the X plane of the dendrite but not the axon over the time course of the experiment. See also Movie S1. Movie S2 shows axonal exclusion of TfRYFP.

(C, D) Single frames from Movie S3 (top) and kymographs (bottom) of TfR-GFP-containing particles moving along 50 μm of Tau-CFP-positive axons in neurons (DIV10) co-expressing mCherry-tagged μ1A-WT or μ1A-W408S. Lines with negative (blue) and positive (red) slopes in the kymographs rep resent particles moving in anterograde and retrograde directions, respectively. Vertical lines represent particles that are stationary during 30 s of recording.

(E) Quantification of the number of TfR-GFP-containing particles per 100 μm of axon in 30 s of recording time. Ant: anterograde, Ret: retrograde, Stat: stationary. Values are mean ± SD of the number of particles (n_p) indicated in the figure. (*) $p<0.01$.

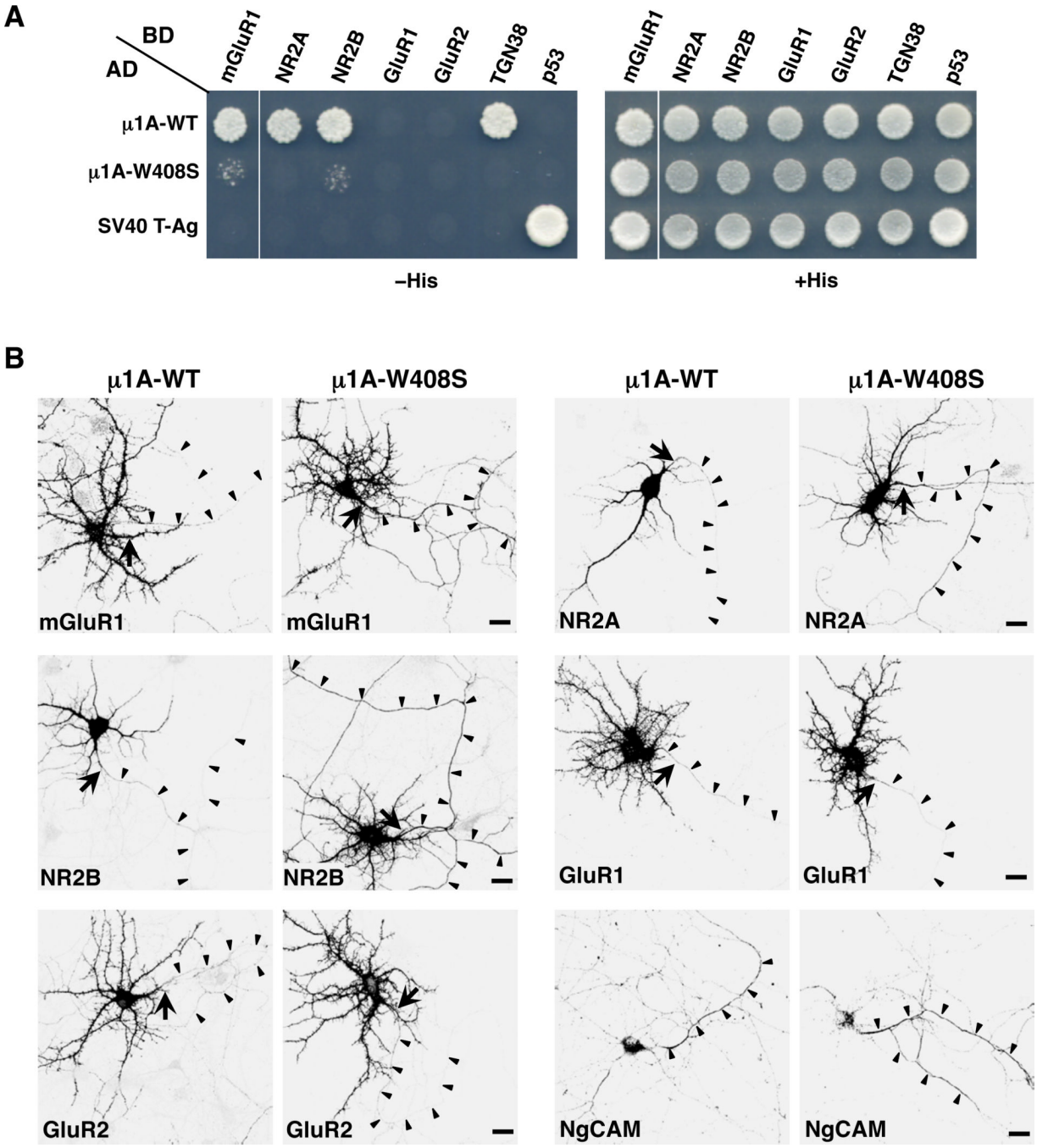

Figure 6. Interaction with μ1A is required for somatodendritic sorting of neuronal glutamate receptor proteins

(A) Y2H analysis of the interaction of the cytosolic domains of mGluR1 (residues 841–1199), NR2A (1304–1464), NR2B (1315–1484), GluR1 (827–906), GluR2 (834–883) or TGN38 (324–353) (positive control) with WT or W408S mutant forms of μ1A, performed as described in the legend to Figure 2B.

(B) Neurons (DIV10) co-expressing combinations of GFP-tagged mGluR1, NR2A, NR2B or GluR1, super-ecliptic pHluorin (SEP)-tagged GluR2 or untagged NgCAM with HA-tagged μ1A-WT or μ1A-W408S were immunostained for the HA epitope and Ank-G. The GFP or SEP signal was enhanced by immunostaining with antibody to GFP. NgCAM was

also detected by immunostaining. GFP, SEP and NgCAM immunostaining is shown in these panels and the corresponding immunostaining for HA and Ank-G is shown in Figure S4C. The distribution of all glutamate receptor proteins and NgCAM is shown in grayscale negative images. Arrow points to the AIS and arrowheads to the axon in each neuron. Scale bars: 20 μm.

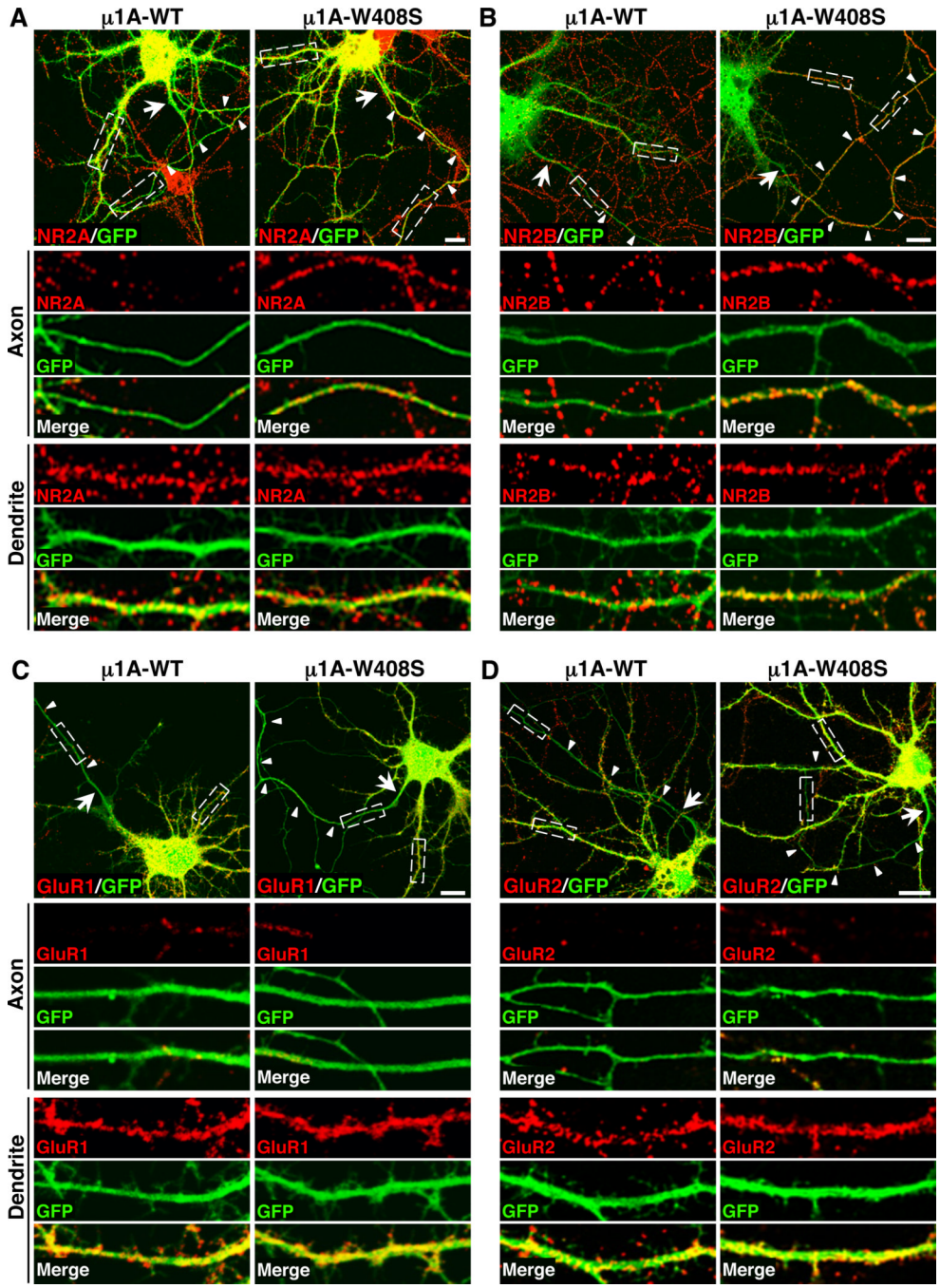

Figure 7. Axonal missorting of endogenous glutamate receptor proteins upon disruption of interactions with μ1A

(A–D) Neurons (DIV10) co-expressing transgenic GFP with HA-tagged μ1A-WT or μ1A-W408S were immunostained for the HA epitope, Ank-G and the endogenous glutamate receptor proteins NR2A (A), NR2B (B), GluR1 (C) and GluR2 (D). Top panels show merged images of GFP (green) and glutamate receptor proteins (red) in cells expressing HA-tagged μ1A constructs. Arrow points to the AIS and arrowheads indicate the axon of each transfected neuron. Images of axons (middle panels) and dendrites (bottom panels) magnified 5X from boxes in the top panels are also shown. Yellow in the merged images indicates co-localization. Scale bars: 10 μm.

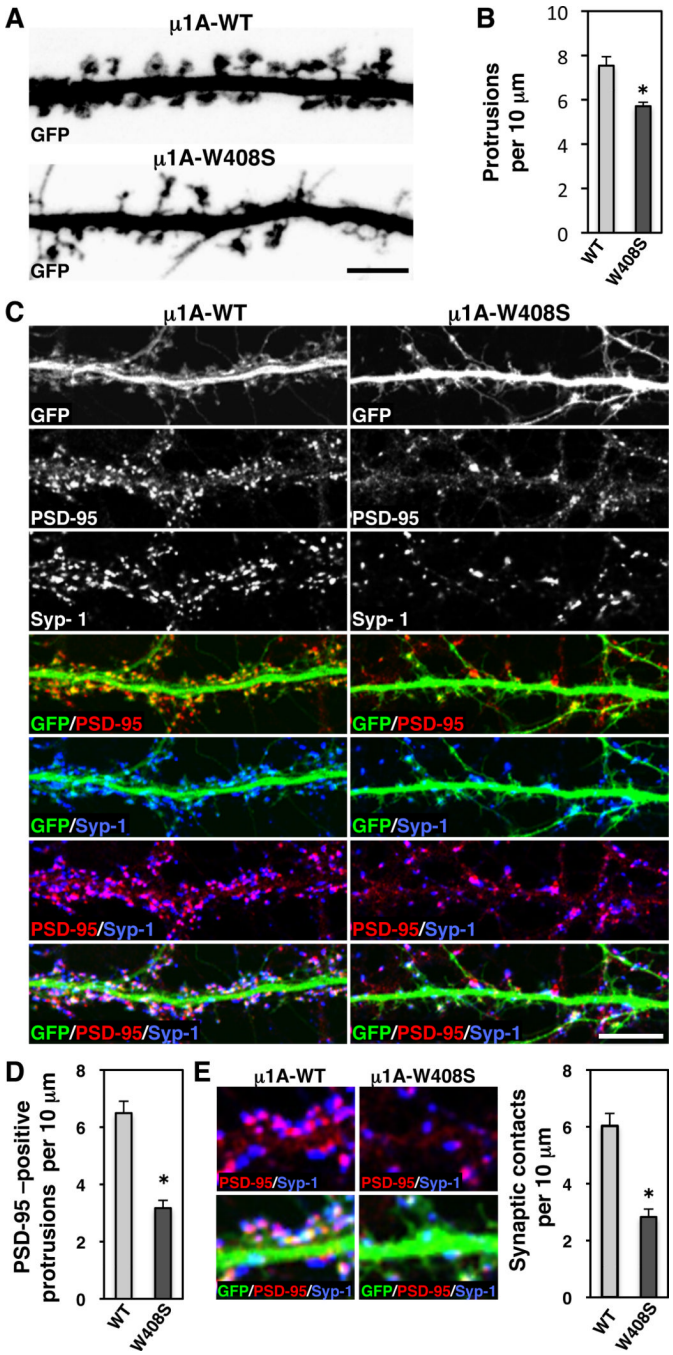

Figure 8. Impaired spine maturation and decreased number of synapses caused by disruption of signal-recognition by μ1A

(A) Z-stack reconstruction of GFP-positive dendrites (grayscale negative) of neurons (DIV18) co-expressing GFP with HA-tagged μ1A-WT or μ1A-W408S.

(B) Quantification of the protrusion density per 10 μm of GFP-positive dendrite length.

(C) Dendrites from neurons (DIV18) co-expressing transgenic GFP (grayscale and green in merges) with HA-tagged μ1A-WT or μ1A-W408S were stained the excitatory postsynaptic PSD-95 (grayscale and red in merges) and the presynaptic synapsin-1 (Syp-1) (grayscale and blue in merges) markers. Scale bars: 5 μm.

(D, E) Quantification of the protrusions immunoreactive for PSD-95 and synaptic contacts per 10 μm of GFP-positive dendrite length. Images in E (left) show higher magnification of synaptic contacts, observed as apposition of PSD95 (red) and synapsin-1 (blue) in GFP-positive dendrite. In all bar graphs (*) $p<0.01$.

Table 1

Quantification of polarity of dendritic and axonal proteins

Transfected	Dendrite:Axon Polarity Index	
TfR-GFP WT	9.1 ± 3.0 (25)	
TfR-GFP Y20A	1.3 ± 0.2 (25)#	
TfR-GFP F23A	1.4 ± 0.2 (25)#	
TfR-GFP WT+ p CD M 8	9.6 ± 3.8 (30)	
TfR-GFP WT + pCMD8-Hub	1.6 ± 0.5 (30) *	
m Cherry-Tubulin	1.2 ± 0.2 (30)	
GFP	1.2 ± 0.2 (25)	
Transfected	µlA-WT	µlA-W408S
TfR-GFP WT	8.1 ± 2.6 (30)	1.3 ± 0.3 (30) *
mGluR1-GFP	9.0 ± 2.7 (35)	1.6 ± 0.4 (35) *
NR2A-GFP	6.3 ± 2.2 (30)	1.4 ± 0.4 (30) *
NR2B-GFP	9.6 ± 2.6 (27)	1.3 ± 0.3 (33) *
GluR1-GFP	8.1 ± 2.0 (25)	7.8 ± 2.0 (30)
SEP-GluR2	7.0 ± 1.4 (30)	6.9 ± 2.8 (28)
NgCAM	0.1 ± 0.1 (30)	0.1 ± 0.1 (30)
Endogenous	µlA-WT	µlA-W408S
NR2A	11.8 ± t 2.7 (30)	1.3 ± 0.2 (40) *
NR2B	8.9 ± 2.1 (30)	1.1 ± 0.3 (35) *
GluR1	7.7 ± 1.3 (30)	6.9 ± 2.2 (30)
GluR2	6.6 ± 1.5 (30)	6.2 ± 1.8 (30)
MAP2	14.4 ± t 2.6 (30)	13.7 ± 2.4 (30)

Values are expressed as mean ± SD *(n)*

(*n*) Number of cells analyzed.

Significantly different from TfR-GFP WT (p<0 .01)

* Significantly different from control group (p<0.01)

Polarity index was calculated as described in Experimental Procedures